Self-sustaining thermophotonic circuits

Bo Zhao[a,b], Siddharth Buddhiraju[a,b], Parthiban Santhanam[a,b], Kaifeng Chen[a,b,c], and Shanhui Fan[a,b,1]

[a]Department of Electrical Engineering, Stanford University, Stanford, CA 94305; [b]Ginzton Laboratory, Stanford University, Stanford, CA 94305; and [c]Department of Applied Physics, Stanford University, Stanford, CA 94305

Edited by Alexis T. Bell, University of California, Berkeley, CA, and approved April 30, 2019 (received for review March 22, 2019)

Photons represent one of the most important heat carriers. The ability to convert photon heat flow to electricity is therefore of substantial importance for renewable energy applications. However, photon-based systems that convert heat to electricity, including thermophotovoltaic systems where photons are generated from passive thermal emitters, have long been limited by low power density. This limitation persists even with near-field enhancement techniques. Thermophotonic systems, which utilize active photon emitters such as light-emitting diodes, have the potential to significantly further enhance the power density. However, this potential has not been realized in practice, due in part to the fundamental difficulty in thermodynamics of designing a self-sustaining circuit that enables steady-state power generation. Here, we overcome such difficulty by introducing a configuration where the light-emitting diodes are connected in series, and thus multiple photons can be generated from a single injected electron. As a result we propose a self-sustaining thermophotonic circuit where the steady-state power density can exceed thermophotovoltaic systems by many orders of magnitude. This work points to possibilities for constructing heat engines with light as the working medium. The flexibility of controlling the relations between electron and photon flux, as we show in our design, may also be of general importance for optoelectronics-based energy technology.

thermophotonics | thermodynamics | electronic circuits | renewable energy

A thermophotonic system, introduced by Green over 20 y ago, is a photon-based thermal energy conversion system that converts heat to electricity (1–8). This system consists of a light-emitting diode (LED) at the hot side and a photovoltaic (PV) cell at the cold side. The emission from the LED is absorbed by the PV cell which produces electricity (Fig. 1*A*). Compared with the standard thermophotovoltaic system (Fig. 1*B*) (9–21), which uses a passive thermal emitter on the hot side, a thermophotonic system can achieve much higher power density if a positive bias is applied on the LED (Fig. 1*A*) (2, 6, 8).

To apply a positive bias on the LED, at least in principle one can assume that the LED is driven by an external battery as shown in Fig. 1*A*. In most theoretical analysis of thermophotonic systems, one further assumes that the battery can somehow be recharged using the electricity produced in the PV cell (4–6). The net output of a thermophotonic system is then computed by taking the output power of the PV cell minus the power that is required to charge the battery (8). However, the round-trip efficiency of battery storage system is about 95% with lithium-ion batteries, and is in the range of 75–80% for many other practical battery systems (22). Even assuming a 95% round-trip efficiency, the use of battery alone would have resulted in the reduction of the efficiency of a thermophotonic system by 5%, which is substantial. In addition, in a battery-driven thermophotonic system, the battery attached to the LED needs to provide a continuous driving power to the LED, and thus will need to be periodically replaced when its energy is drained. In practice, this also adds significantly to the complexity and potentially the cost of the overall system. It would be far more attractive if one can design a circuit such that part of the electricity produced by the PV cell can be used to directly provide the positive bias on the LED. In this paper, we refer to such a circuit as a self-sustaining thermophotonic circuit. In a self-sustaining circuit, at steady state, the LED should be positively biased, and the PV cell should operate in the photovoltaic mode, i.e., it should also be positively biased with a negative current that flows through the PV cell. Remarkably, even though the concept of thermophotonic system was introduced over 20 y ago, there has not been any conceptual design of a self-sustaining thermophotonic circuit. Previously analysis of a thermophotonic circuit has instead highlighted some of the conceptual difficulties of analyzing and constructing such a self-sustaining circuit (4, 7).

In this paper, we provide an analysis of the difficulties in previous works for constructing a self-sustaining thermophotonic circuit, and, based on this analysis, we introduce a design of a self-sustaining circuit. We show that the key to constructing such a circuit is the use of a series connection of multiple LEDs, such that each injected electron can produce multiple photons. The resulting thermophotonic system can enhance steady-state power density to a level that is orders of magnitude above corresponding thermophotovoltaic systems, with comparable efficiency. Such enhancement moreover can be achieved either in near-field or far-field systems. Therefore, we believe that such a self-sustaining thermophotonic circuit will be important for a number of applications such as solar energy harvesting (2) and waste-heat recovery (8). The realization that the electron and photon flux need not be strictly equal even in ideal systems, as we show in our design, may also point to previously unexplored flexibilities in designing optoelectronic devices for energy applications.

Analysis of Previous Attempts

We start by reanalyzing previous attempts (4, 7) in designing a thermophotonic circuit with one LED and one PV cell surrounded by an environment, to highlight the difficulties for constructing a

Significance

Photon-based systems that convert heat to electricity have been limited by low power density. Thermophotonic systems have the potential to significantly enhance the power density. This potential has not been realized in practice, due in part to the fundamental thermodynamic difficulty in designing a self-sustaining circuit that enables steady-state power generation. Current construction instead uses batteries which lower system efficiency and adds complexity. We overcome such difficulty by introducing an electronic circuit where multiple photons can be generated from a single electron. Our design enables a self-sustaining thermophotonic circuit that can achieve a steady-state power density exceeding traditional thermophotovoltaic systems by many orders of magnitude. This work highlights possibilities for constructing heat engines with light as the working medium.

Author contributions: B.Z. and S.F. designed research; B.Z. performed research; B.Z., S.B., P.S., K.C., and S.F. analyzed data; and B.Z. and S.F. wrote the paper.

The authors declare no conflict of interest.

This article is a PNAS Direct Submission.

[1]To whom correspondence may be addressed. Email: shanhui@stanford.edu.

This article contains supporting information online at www.pnas.org/lookup/suppl/doi:10.1073/pnas.1904938116/-/DCSupplemental.

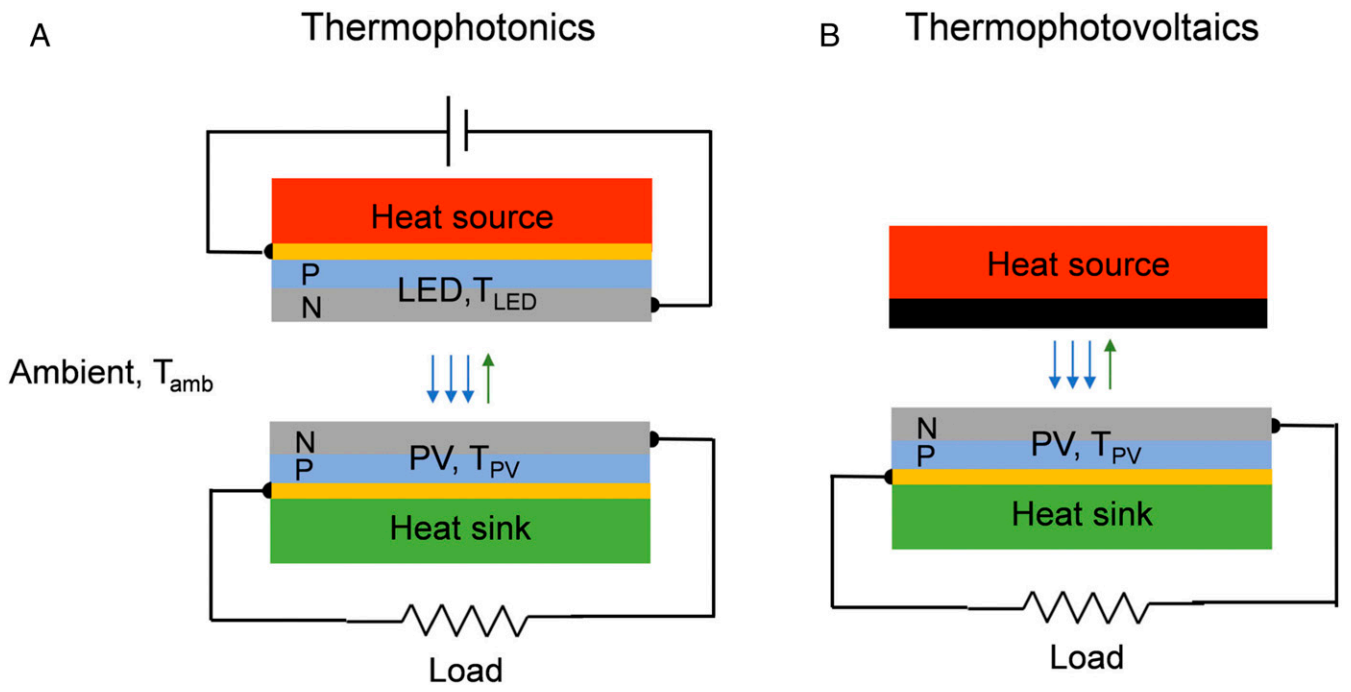

Fig. 1. (*A*) Schematic of a thermophotonic system using batteries. The battery connected to the LED is used to drive the LED. The battery connected to the PV cell is charged by the PV cell. (*B*) Schematic of a TPV system. The black region is a blackbody thermal emitter, and there is no filter in this TPV system. In both *A* and *B*, the regions immediately above the PV cell are vacuum gaps. The yellow regions are back reflectors that are assumed to be a perfect mirror.

self-sustaining thermophotonic circuit. The geometry is the same as in Fig. 1*A* without any assumption on the external circuits. We denote the temperatures of the LED, the PV cell, and the ambient as T_{LED}, T_{PV}, and T_{amb}, respectively. We assume the emission from the LED and the PV cell is above their respective bandgaps. In other words, the below-bandgap emissivity is assumed to be zero. To operate this system as a thermophotonic circuit for the purpose of thermal energy harvesting, we assume $T_{\mathrm{LED}} > T_{\mathrm{PV}} \geq T_{\mathrm{amb}}$. We assume that one photon produces one electron–hole pair in the PV cell and vice versa in the LED regardless of the energy of the photon. We also assume the only radiative recombination of importance is direct recombination between free holes and electrons. For the voltage and current of the LED and PV cell, we choose a sign convention such that a positive current flows from the P to the N region internally. And, a positive voltage corresponds to a higher voltage on the P region. Under this convention, at steady state, a self-sustaining thermophotonic circuit should have positive voltages on both the LED and the PV cell, i.e., $V_{\mathrm{LED}} > 0$ and $V_{\mathrm{PV}} > 0$. The current I_{LED} through the LED should be positive, and the current density I_{PV} through the PV cell should be negative in order for the PV cell to operate in the PV mode and generate power.

From the detailed balance analysis (23), we can obtain the current in the LED (I_{LED}) and PV cell (I_{PV})

$$[F_{\mathrm{amb}\to\mathrm{LED}} - F_{\mathrm{LED}\to\mathrm{amb}}] + [F_{\mathrm{PV}\to\mathrm{LED}} - F_{\mathrm{LED}\to\mathrm{PV}}] + [N_{\mathrm{LED}}(0) - N_{\mathrm{LED}}(V_{\mathrm{LED}})] + \frac{I_{\mathrm{LED}}}{q} = 0, \quad [1]$$

and

$$[F_{\mathrm{amb}\to\mathrm{PV}} - F_{\mathrm{PV}\to\mathrm{amb}}] + [F_{\mathrm{LED}\to\mathrm{PV}} - F_{\mathrm{PV}\to\mathrm{LED}}] + [N_{\mathrm{PV}}(0) - N_{\mathrm{PV}}(V_{\mathrm{PV}})] + \frac{I_{\mathrm{PV}}}{q} = 0. \quad [2]$$

In the above two equations, $F_{a\to b}$ is the photon flux emitted by object a and received by object b, where a, b = PV, LED, and the ambient. $N(0)$ and $N(V)$ are the nonradiative generation and recombination rates of the electron–hole pairs, respectively, and q is the unit electrical charge. Adding Eqs. **1** and **2**, we have

$$-\frac{I_{\mathrm{LED}} + I_{\mathrm{PV}}}{q} = [F_{\mathrm{amb}\to\mathrm{LED}} - F_{\mathrm{LED}\to\mathrm{amb}}] + [N_{\mathrm{LED}}(0) - N_{\mathrm{LED}}(V_{\mathrm{LED}})] + [F_{\mathrm{amb}\to\mathrm{PV}} - F_{\mathrm{PV}\to\mathrm{amb}}] + [N_{\mathrm{PV}}(0) - N_{\mathrm{PV}}(V_{\mathrm{PV}})]. \quad [3]$$

On the other hand, suppose the circuit is self-sustaining; we have $V_{\mathrm{LED}} > 0$ and $V_{\mathrm{PV}} > 0$. Hence each term in a bracket on the right-hand side of Eq. **3** is negative. Thus, for a self-sustaining circuit involving one LED and one PV cell, we must have

$$I_{\mathrm{LED}} + I_{\mathrm{PV}} > 0. \quad [4]$$

In the limit where V_{LED} and V_{PV} are large compared with the relevant temperatures, Eq. **4** can be intuitively understood since in that limit each electron produced by the PV cell must arise from a photon emitted by the LED. And, each injected electron into the LED at most can produce one photon. The proof of Eq. **4** however is rigorous and does not rely upon such intuition. We also note that the derivation above is very general. The main assumptions about the LED and PV cell are the same as those in the Shockley–Queisser analysis of solar cells (23). The derivation makes no assumption about either the optical or the electronic setup of the system. Neither does the derivation assume reciprocity.

The current constraint in Eq. **4** makes it difficult to construct a self-sustaining circuit using one LED and one PV cell. To illustrate this difficulty, we consider two types of circuits. The first one is shown in Fig. 2*A*. The circuit consists of an LED, a PV cell, and a load resistor, all connected in series. The load has a resistance R. For this circuit, Kirchhoff's circuit law requires $I_{\mathrm{LED}} = -I_{\mathrm{PV}}$, which conflicts with Eq. **4**. Therefore, at steady state, V_{LED} and V_{PV}

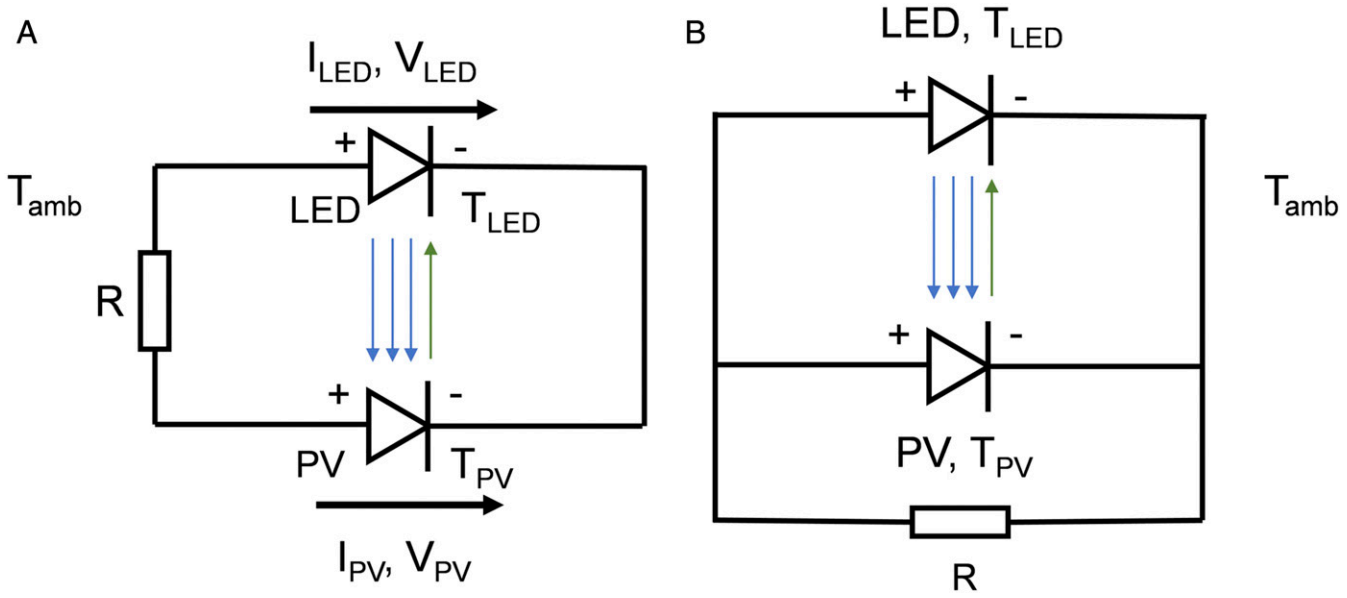

Fig. 2. (*A*) Circuit where a resistor is connected in series with the LED and PV cell. (*B*) Circuit where a resistor is connected in parallel with the PV cell and the LED. The load is represented by a resistor with a resistance *R*. The temperatures of the LED and the PV cell are T_{LED} and T_{PV}, respectively, and $T_{LED} > T_{PV}$.

cannot be both positive, thus the circuit in Fig. 2*A* cannot be a self-sustaining thermophotonic system. In *SI Appendix*, we further show that $V_{LED} < 0$, which agrees with Green's result (4). Similarly, one can show the circuit shown in Fig. 2*B*, where the PV cell and the resistor are in a parallel configuration, also cannot operate self-sustainingly since the circuit requires $-I_{PV} = I_{LED} + V_{LED}/R$, which also conflicts with Eq. **4**.

As a side note, in the ideal case where the ambient photon fluxes and the nonradiative terms are both neglected, from a system of equations consisting of Eqs. **1** and **2** as well as the equations from the circuit law, one can show that the steady state of the circuits in Fig. 2*B* is $V_{PV} = V_{LED} = 0$. On the other hand, for the circuit in Fig. 2*A*, its system of equations in fact admits an infinite number of possible steady-state solutions. Green (4) proposed that the physical steady state of this system should be derived invoking additional constraints provided by the principles of minimum entropy production, but did not give a detailed derivation. In *SI Appendix*, we provide a derivation to obtain the steady state in this ideal case. Our derivation does not use the principle of minimum entropy production, but instead treats the ideal case as the limiting case where the nonradiative recombination rates approach zero.

Proposed Circuit

From the intuitive argument of Eq. **4**, then, the key toward creating a self-sustaining circuit is to decouple the number of injected electrons to the LED and the number of photons generated. For this purpose, we propose a circuit as shown in Fig. 3*A*. Compare with the geometry in Fig. 2*B*, in this system, on the hot side, we have $N > 1$ number of LEDs connected in series, and on the cold side, we have $M \geq 1$ number of PV cells connected in series. The key in this circuit is that each electron passing through the LEDs can produce multiple photons. Below, we will show that such a circuit becomes self-sustaining with $N > M$.

For the circuit in Fig. 3*A*, since the LEDs and the PV cells are connected in series, all of the LEDs and all of the PV cells have the same currents. We denote the currents passing through the LEDs and the PV cells as I_{LED} and I_{PV}, respectively. We also denote the voltage on the *i*th PV cell and the *j*th LED as $V_{PV,i}$ and $V_{LED,j}$, respectively. The Kirchhoff circuit laws then result in

$$\sum V_{PV,i} = \sum V_{LED,j}, \quad [5]$$

$$\sum V_{LED,j} = R(-I_{PV} - I_{LED}). \quad [6]$$

Additional equations can be obtained based on detailed balance. For simplicity, we first assume that the LEDs and PV cell are ideal with no nonradiative recombination. We also make the assumptions that all LEDs and PV cells have unity emissivity above the bandgap and zero emissivity below. The view factors between the LEDs and the PV cells are such that there is no photon exchange with the ambient. With these assumptions, we obtain the currents in the PV cells and the LEDs as

$$\frac{I_{PV}}{q} = \sum_j \left(F_{PV,i\to LED,j} - F_{LED,j\to PV,i}\right) + \sum_h \left(F_{PV,i\to PV,h} - F_{PV,h\to PV,i}\right), \quad [7]$$

and

$$\frac{I_{LED}}{q} = \sum_i \left(F_{LED,j\to PV,i} - F_{PV,i\to LED,j}\right) + \sum_h \left(F_{LED,j\to LED,h} - F_{LED,h\to LED,j}\right), \quad [8]$$

respectively. $F_{a\to b}$ is the photon flux emitted by device *a* and received by device *b*, and has the form

$$F_{a\to b}(T_a, V_a) = A_a f_{a\to b} F_0(T_a, V_a) \quad [9]$$

In Eq. **9**, A_a is the surface area of device *a*, and $f_{a\to b}$ is the view factor from device *a* to device *b*. $F_0(T_a, V_a)$ is the emitted photon flux density of device *a* to all directions (4, 24–27):

$$F_0(T_a, V_a) = \int_{\omega_g}^{\infty} \frac{\omega^2}{4\pi^2 c^2} \frac{1}{\exp\left(\frac{\hbar\omega - qV_a}{k_B T_a}\right) - 1} d\omega. \quad [10]$$

In the above equation, ω is the angular frequency and ω_g is the frequency corresponding to the bandgap (E_g), k_B is the Boltzmann

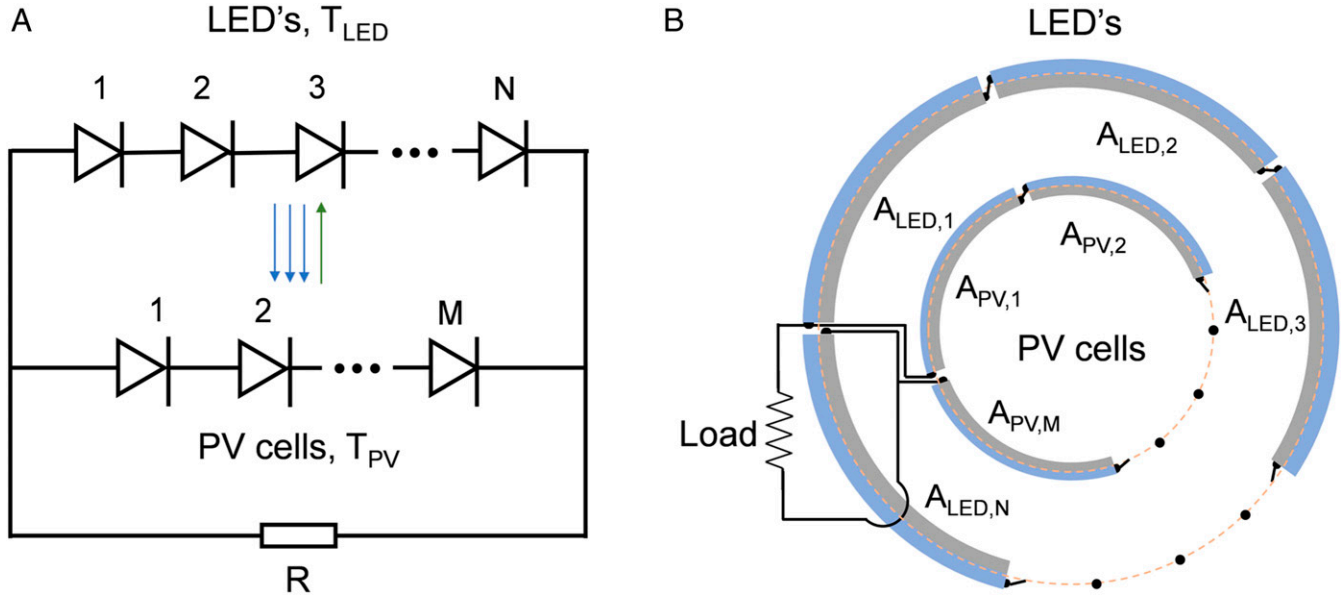

Fig. 3. (*A*) Proposed thermophotonic circuit that uses multiple LEDs (*N* in total) and multiple PV cells (*M* in total). We assume $N > M$. The load is a resistor with a resistance *R*. (*B*) Schematic of the physical connections of the LEDs, PV cells, and the load, with the LEDs and the PV cells arranged in the symmetric configuration. The areas of each PV cell and LED are $A_{PV,i}$, and $A_{LED,j}$, respectively, with $i = 1,2,\ldots M$, and $j = 1,2,\ldots N$.

constant, $\hbar$ is the reduced Planck constant, c is the speed of light in vacuum. When $\hbar\omega_g - qV_a > 3k_BT_a$, we can approximate the Bose–Einstein distribution with a Boltzmann distribution (4, 23):

$$F_0(T_a, V_a) = F_0(T_a, 0)\exp\left(\frac{V_a}{V_{th,a}}\right). \quad [11]$$

In Eq. **11**, $V_{th,a} = k_BT_a/q$. Eqs. **5**–**8** can be used to solve for the voltages for all LEDs and PV cells.

The solution of Eqs. **5**–**8** in a general situation can be very complicated due to the nonlinear nature of the system. Instead, below we provide the solution of Eqs. **5**–**8** for a specific system to show that a self-sustaining thermophotonic circuit indeed can be realized with this class of circuit. The system is shown in Fig. 3*B*, where all LEDs are the same and so are all PV cells. We assume that the LEDs and the PV cells have the same bandgap at their respective temperatures. The LEDs and the PV cells are arranged in a symmetric configuration. By symmetry then, all of the LEDs have the same voltage V_{LED}, and all of the PV cells have the same voltage V_{PV}. Eqs. **5**–**8** thus simplify to

$$MV_{PV} = NV_{LED}, \quad [12]$$

$$NV_{LED} = R(-I_{PV} - I_{LED}), \quad [13]$$

$$\frac{I_{PV}}{q} = A_{PV}[F_0(T_{PV}, V_{PV}) - F_0(T_{LED}, V_{LED})]. \quad [14]$$

and

$$\frac{I_{LED}}{q} = \frac{M}{N}A_{PV}[F_0(T_{LED}, V_{LED}) - F_0(T_{PV}, V_{PV})]. \quad [15]$$

In Eqs. **14** and **15**, A_{PV} is the area of a PV cell. Eqs. **14** and **15** can be derived assuming reciprocity, as detailed in *SI Appendix*. We note that the area of the LED does not affect the performance of the system due to reciprocity. We see that when $N > M$, the photon flux injected into a PV cell, $A_{PV}[F_0(T_{LED}, V_{LED}) - F_0(T_{PV}, V_{PV})]$, exceeds the electron flux injected into the LEDs, $\frac{M}{N}A_{PV}[F_0(T_{LED}, V_{LED}) - F_0(T_{PV}, V_{PV})]$. Thus, $-I_{PV} > I_{LED}$, and hence part of the current generated by the PV cell can be used to drive the external load, which is the key for a self-sustaining circuit. From Eqs. **12**–**15**, we obtain an implicit equation for V_{LED}:

$$\frac{N^2V_{LED}}{qRA_{PV}} = (N-M)\left[F_0(T_{LED}, 0)\exp\left(\frac{V_{LED}}{V_{th,LED}}\right) - F_0(T_{PV}, 0)\exp\left(\frac{N}{M}\frac{V_{LED}}{V_{th,PV}}\right)\right]. \quad [16]$$

Since $T_{LED} > T_{PV}$, $V_{th,LED} > V_{th,PV}$, and $F_0(T_{LED}, 0) > F_0(T_{PV}, 0)$, for any value of *R*, Eq. **16** has a unique solution in the range of $V_{LED} > 0$. Thus, we prove that the circuit is self-sustaining when $N > M$. We note that the Boltzmann approximation is used in deriving the above equation to simplify the analytic calculation. One can use the Bose–Einstein distribution and obtain the same conclusion. Since the Bose–Einstein distribution is valid for all voltages, we will use the Bose–Einstein distribution in the following calculations. We also note that in above derivations we assume the emission from LEDs and PV cells is Lambertian. If the emission is not Lambertian, one would need to do an integration over angle to compute the photon flux. The rest of the analysis proceeds similarly. The main conclusion of the paper, that a self-sustaining circuit requires a different number of LEDs and PV cells, remains unchanged.

Performance of the Proposed Circuit

To illustrate the detailed performance of the circuit shown in Fig. 3*B*, we now present a specific example, where the LEDs are at a temperature of 600 K, and the PV cells are at 300 K. We set the bandgaps of the LEDs and the PV cell to be 1.64 eV, which can be achieved using AlGaAs compounds. These settings are the same as the thermophotonic system used in ref. 8 for high-performance waste-heat recovery. The electric power density is calculated with respect to the total area of the PV cells.

For comparison, we note that, assuming only far-field radiation, a thermophotovoltaic system with a blackbody emitter at a temperature of 600 K, and a PV cell at 300 K, achieves a maximum electric power and the maximum efficiency of 28.6 pW/cm^2 and 47.63%, respectively.

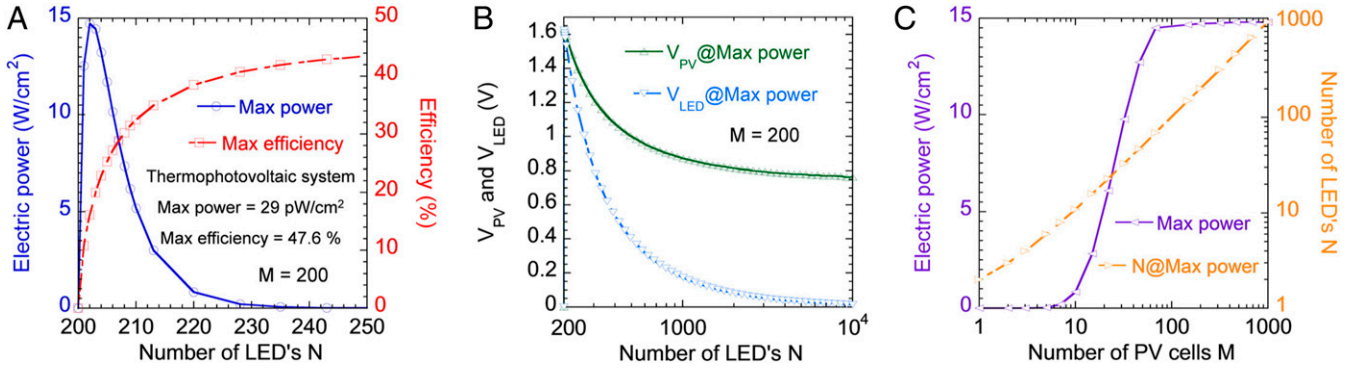

Fig. 4. (*A*) Maximum electric power and maximum efficiency of the proposed thermophotonic circuit, as a function of the number of LEDs. The number of PV cells is fixed at $M = 200$. (*B*) Voltages of the PV cell and the LEDs at maximum electric power points as a function of the number of LEDs. The number of PV cells is fixed at $M = 200$. (*C*) Maximum electric power and the number of the LEDs at each maximum power point as a function of the number of the PV cells.

We first discuss a specific case where the number of the PV cells is fixed at $M = 200$. For the proposed thermophotonic circuit, Fig. 4*A* shows the maximum electric power and maximum efficiency of the circuit as the number of the LEDs N increases. N needs to be greater than M for the circuit to be a self-sustaining thermophotonic system. For each $N > 200$, we find the maximum power point and the maximum efficiency point by optimizing the load resistance R. At $N = 200$, the circuit generates no power. The power peaks at $N = 202$ and then decreases when N becomes larger. The peak electric power, 14.73 W/cm^2, is more than 11 orders of magnitude larger than the maximum power of the corresponding thermophotovoltaic system with the same temperatures. Such a very substantial power density is achieved entirely with far-field radiation, and points to the significant capability for power density enhancement in thermophotonics compared with thermophotovoltaics.

In the comparison with thermophotovoltaic system above, the corresponding thermophotovoltaic system uses the same semiconductor and operates in the far field. We consider such a thermophotovoltaic system, even though it is not optimal in terms of power density, since it highlights the difference between the concepts of thermophotonics and thermophotovoltaics. In *SI Appendix*, we consider instead the performance of an optimal near-field thermophotovoltaic (TPV) system using a plasmonic emitter with the surface plasmon frequency matching the bandgap of a narrow-bandgap semiconductor (20, 28). Such an optimal near-field TPV system can reach a power density of 14.4 W/cm^2 when the vacuum gap size is at 10 nm. Our thermophotonic circuits outperform such power density when operating in the far field. By operating our thermophotonic circuits in the near field, one can further enhance its power density to 114 W/cm^2, as shown in *SI Appendix*. Therefore, our thermophotonic circuit indeed can significantly outperform the optimal TPV system in terms of power density.

As the number of LEDs N increases significantly beyond the number of PV cells, the electric power decreases and asymptotically approaches the power of the corresponding TPV case, as shown in Fig. 4*A*. In Fig. 4*B*, we show the voltages of the LEDs and PV cells at the maximum power points as N increases. We see that V_{LED} approaches zero when N becomes large. In this case the LEDs operate as a thermal emitter at equilibrium and hence the system becomes the same as the TPV system. Both the power density and V_{PV} thus approach that of the TPV system.

In general, the efficiency of the thermophotonic system falls below that of the TPV system, since part of the power generated by the PV cell needs to be used to drive the LEDs. Therefore, the maximum efficiency of the system increases as the number of LED N increases and also approaches the TPV case at the large-N limit, as shown in Fig. 4*A*. The key advantage of the thermophotonic circuit is to achieve orders of magnitude enhancement of the power density while maintaining a reasonable system efficiency. For example, at the peak power density of 14.73 W/cm^2 with $M = 200$ and $N = 202$, the system efficiency remains relatively high at 16.14%. We note that, since the voltage-enhanced effect is primarily just above the bandgap, the high-intensity emission naturally has wavelength selectivity. This selectivity could help to mitigate the effect of the parasitic subbandgap emission from the emitter (1, 2), which is typically achieved by photon recycling design in TPVs.

Fig. 4*C* shows the maximum electric power when the number of the PV cells changes. For each specific number of PV cells, we find the maximum power point by optimizing the load resistor R and the number of the LEDs. We find that the maximum power point increases as the number of the PV cells increases, and approaches 14.8 W/cm^2 when $M > 70$. This power density is the maximum power density that the system can reach. Fig. 4*C* also shows the number of the LEDs needed at each maximum power point. We note that the ratio of the number of the PV cells and the LEDs is very close to 1, i.e., M: $N \approx 1$. The radiation power density of an LED increases drastically when V_{LED} is close to the bandgap (8). On the other hand, V_{PV} needs to be greater than V_{LED} since $M < N$. However, both V_{PV} and V_{LED} need to remain smaller than the bandgap, since otherwise the system would be dominated by stimulated emission processes. Therefore, at the peak power points, V_{PV} and V_{LED} are both close to the bandgap with V_{PV} being slightly larger than V_{LED}, resulting in M: $N = V_{\mathrm{LED}}$: $V_{\mathrm{PV}} \approx 1$.

We now briefly comment on the effects of nonradiative recombination and incomplete light exaction in the circuit of Fig. 3. Defining the external quantum efficiencies of the LEDs and PV cells as

$$\eta_{\mathrm{PV}} = \frac{-I_{\mathrm{PV}}/q}{A_{\mathrm{PV}} F_0(T_{\mathrm{LED}}, V_{\mathrm{LED}})}, \qquad [17]$$

and

$$\eta_{\mathrm{LED}} = A_{\mathrm{PV}} \frac{M}{N} \frac{F_0(T_{\mathrm{LED}}, V_{\mathrm{LED}})}{I_{\mathrm{LED}}/q}, \qquad [18]$$

η_{PV} and η_{LED} fall below unity in the presence of either effect. Since the PV cells need to produce more power than what is consumed in the LEDs, one needs to have $MI_{\mathrm{PV}}V_{\mathrm{PV}} + NI_{\mathrm{LED}}V_{\mathrm{LED}} < 0$. Using Eqs. **12**, **17**, and **18**, in order for the circuit of Fig. 3 to produce power, we must have

$$\eta_{\mathrm{PV}}\eta_{\mathrm{LED}} > \frac{M}{N}. \qquad [19]$$

Since $M/N = V_{\mathrm{LED}}/V_{\mathrm{PV}} > qV_{\mathrm{LED}}/E_{\mathrm{g}}$, Eq. **19** implies $\eta_{\mathrm{LED}} > qV_{\mathrm{LED}}/E_{\mathrm{g}}$, which is the condition for electroluminescent refrigeration

using LEDs (29). Therefore, the operation of the thermophotonic circuit here is closely related to the concept of electroluminescent refrigeration. The required external quantum efficiencies for the circuit to generate power decreases as M/N gets smaller. For example, at the peak power point, $M = 200$ and $N = 202$, the required external quantum efficiencies for both LEDs and PV cells need to be greater than 99%, and this number decreases to about 90% if N increases to 220. The maximum power density the system can achieve also drops as the external quantum efficiencies decrease. For example, with the external quantum efficiencies for both LEDs and PV cells being 98%, the maximum power density decreases to 1.1 W/cm^2, achieved at $M = 200$ and $N = 212$. We note that using our proposed circuit has the same requirement for high external quantum efficiency compared with the systems that use batteries. Therefore, high-performance LEDs in elevated temperatures, which are essential for the experimental demonstration of thermophotonic system, are also required for our self-sustaining circuits. In this context, we believe that our work provides additional motivation for improving LED performance. In *SI Appendix*, we discuss in detail the effect of the external quantum efficiency on the power density and the efficiency of the system.

We end the paper by discussing some practical considerations. The use of a cylindrical surface is for ease of analysis and is not strictly required in practical systems. The cylindrical configuration is used to ensure that all photons emitted by the LED are absorbed by the PV cells. In practice, any configurations, including planar configurations that satisfy this requirement, should be sufficient. Connecting a substantial number of LEDs or PV cells in series should not be a concern in practice. Practical solar PV systems routinely connect a number of cells in series to achieve a high voltage (30). Our thermal photonic circuit should therefore be scalable in a similar fashion. The practical performance of the system will be limited by a number of loss mechanisms. In addition to the effects of nonradiative recombination and incomplete light extraction as discussed above, other loss mechanisms include the heat conduction through the wires connecting the LEDs and the PV cells, which represents a thermal short between the heat source and the heat sink, as well as the leakage of the photons generated by the LEDs to any absorbers other than the PV cells (8). A high-performance thermophotonic system would require optimization to suppress the contributions of these loss mechanisms. While the analysis in the paper assumes far-field radiation, the same circuit can be applied in near-field systems, with further enhancement of power density. The operation in the near field may also serve to mitigate some of the detrimental effects of nonradiative recombination (8, 25, 27). In summary, we show that a self-sustaining thermophotonic circuit can be constructed, with the potential of significantly enhancing the power density of heat engines that use photons as the working medium.

ACKNOWLEDGMENTS. B.Z. thanks Mr. Cheng Guo and Ms. Zhexin Zhao for discussions. We acknowledge the support from the Global Climate and Energy Project at Stanford University, the Department of Energy "Light-Material Interactions in Energy Conversion" Energy Frontier Research Center under Grant DE-SC0001293, and the Department of Energy "Photonics at Thermodynamic Limits" Energy Frontier Research Center under Grant DE-SC0019140. S.B. acknowledges the support of a Stanford Graduate Fellowship.

1. M. A. Green, Third generation photovoltaics: Ultra-high conversion efficiency at low cost. *Prog. Photovolt. Res. Appl.* **9**, 123–135 (2001).
2. N. P. Harder, M. A. Green, Thermophotonics. *Semicond. Sci. Technol.* **18**, S270–S278 (2003).
3. K. L. Lin, K. R. Catchpole, P. Campbell, M. A. Green, High external quantum efficiency from double heterostructure InGaP/GaAs layers as selective emitters for thermophotonic systems. *Semicond. Sci. Technol.* **19**, 1268–1272 (2004).
4. M. A. Green, *Third Generation Photovoltaics: Advanced Solar Energy Conversion* (Springer Science & Business Media, New York, 2006).
5. B. Heeg, J.-B. Wang, S. R. Johnson, B. D. Buckner, Y.-H. Zhang, Thermally assisted electroluminescence: A viable means to generate electricity from solar or waste heat?, *Proc. SPIE*, **6461**, p. 64610K (2007).
6. B. D. Buckner, B. Heeg, Power generation by thermally assisted electroluminescence: Like optical cooling, but different, *Proc. SPIE*, **6907**, p. 69070I (2008).
7. G. Hatakoshi, "Consideration of wall-plug efficiency for LEDs" in *22nd Microoptics Conference*, The Japan Society of Applied Physics, Ed. (IEEE, Tokyo, Japan, 2017).
8. B. Zhao, P. Santhanam, K. Chen, S. Buddhiraju, S. Fan, Near-field thermophotonic systems for low-grade waste heat recovery. *Nano Lett.* **18**, 5224–5230 (2018).
9. B. D. Wedlock, Thermo-photo-voltaic energy conversion. *Proc. IEEE* **51**, 694–698 (1963).
10. R. M. Swanson, A proposed thermophotovoltaic solar energy conversion system. *Proc. IEEE* **67**, 446–447 (1979).
11. E. Rephaeli, S. Fan, Absorber and emitter for solar thermo-photovoltaic systems to achieve efficiency exceeding the Shockley-Queisser limit. *Opt. Express* **17**, 15145–15159 (2009).
12. W. R. Chan *et al.*, Toward high-energy-density, high-efficiency, and moderate-temperature chip-scale thermophotovoltaics. *Proc. Natl. Acad. Sci. U.S.A.* **110**, 5309–5314 (2013).
13. A. Lenert *et al.*, A nanophotonic solar thermophotovoltaic device. *Nat. Nanotechnol.* **9**, 126–130 (2014).
14. D. M. Bierman *et al.*, Enhanced photovoltaic energy conversion using thermally based spectral shaping. *Nat. Energy* **1**, 16068 (2016).
15. Z. Zhou, E. Sakr, Y. Sun, P. Bermel, Solar thermophotovoltaics: Reshaping the solar spectrum. *Nanophotonics* **5**, 1–21 (2016).
16. Z. Omair *et al.*, "Experimental demonstration of 28.2% thermophotovoltaic conversion efficiency" in *Conference on Lasers and Electro-Optics*, (Optical Society of America, San Jose, CA, 2018), p. AW3O.7.
17. A. Narayanaswamy, G. Chen, Surface modes for near field thermophotovoltaics. *Appl. Phys. Lett.* **82**, 3544–3546 (2003).
18. M. Laroche, R. Carminati, J. J. Greffet, Near-field thermophotovoltaic energy conversion. *J. Appl. Phys.* **100**, 063704–063710 (2006).
19. K. Park, S. Basu, W. P. King, Z. M. Zhang, Performance analysis of near-field thermophotovoltaic devices considering absorption distribution. *J. Quant. Spectrosc. Radiat. Transf.* **109**, 305–316 (2008).
20. O. Ilic, M. Jablan, J. D. Joannopoulos, I. Celanovic, M. Soljačić, Overcoming the black body limit in plasmonic and graphene near-field thermophotovoltaic systems. *Opt. Express* **20**, A366–A384 (2012).
21. A. Fiorino *et al.*, Nanogap near-field thermophotovoltaics. *Nat. Nanotechnol.* **13**, 806–811 (2018).
22. P. Alotto, M. Guarnieri, F. Moro, Redox flow batteries for the storage of renewable energy: A review. *Renew. Sustain. Energy Rev.* **29**, 325–335 (2014).
23. W. Shockley, H. J. Queisser, Detailed balance limit of efficiency of p-n junction solar cells. *J. Appl. Phys.* **32**, 510–519 (1961).
24. P. Wurfel, The chemical potential of radiation. *J. Phys. C Solid State Phys.* **15**, 3967 (1982).
25. K. Chen, P. Santhanam, S. Sandhu, L. Zhu, S. Fan, Heat-flux control and solid-state cooling by regulating chemical potential of photons in near-field electromagnetic heat transfer. *Phys. Rev. B Condens. Matter Mater. Phys.* **91**, 134301 (2015).
26. S. Fan, Thermal photonics and energy applications. *Joule* **1**, 264–273 (2017).
27. K. Chen, T. P. Xiao, P. Santhanam, E. Yablonovitch, S. Fan, High-performance near-field electroluminescent refrigeration device consisting of a GaAs light emitting diode and a Si photovoltaic cell. *J. Appl. Phys.* **122**, 143104 (2017).
28. B. Zhao *et al.*, High-performance near-field thermophotovoltaics for waste heat recovery. *Nano Energy* **41**, 344–350 (2017).
29. T. P. Xiao, K. Chen, P. Santhanam, S. Fan, E. Yablonovitch, Electroluminescent refrigeration by ultra-efficient GaAs light-emitting diodes. *J. Appl. Phys.* **123**, 173104 (2018).
30. L. M. Fraas, L. D. Partain, *Solar Cells and Their Applications* (Wiley & Sons, Hoboken, NJ, 2010).

Supplementary Information for

Self-Sustaining Thermophotonic Circuits

Bo Zhao[1,3], Siddharth Buddhiraju[1,3], Parthiban Santhanam[1,3], Kaifeng Chen[1,2,3], and Shanhui Fan[1,3,a)]

[1]Department of Electrical Engineering
Stanford University, Stanford, California 94305, USA
[2]Department of Applied Physics
Stanford University, Stanford, California 94305, USA
[3]Ginzton Laboratory, Stanford University, Stanford, California 94305, USA

Session I: Steady state of the circuit in Fig. 2a

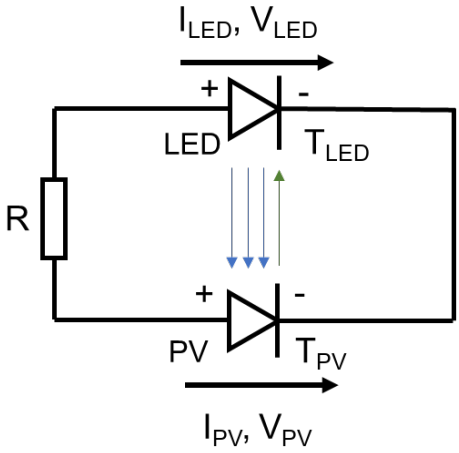

Figure S1. Circuit initially proposed by Green (1) for the thermophotonic system, where a load is connected in series with the LED and PV cell. The load is represented by a resistor with a resistance R. The temperatures of the LED and the PV cell are T_{LED} and T_{PV}, respectively, and $T_{\mathrm{LED}} > T_{\mathrm{PV}}$.

a) Author to whom correspondence should be addressed. Electronic mail: shanhui@stanford.edu

www.pnas.org/cgi/doi/10.1073/pnas.1904938116

We provide a discussion for the steady state of the circuit in Fig. S1. For simplicity, we assume that the LED and the PV cell have the same area. One can obtain two equations based on Kirchhoff's circuit laws,

$$V_{\mathrm{PV}} = I_{\mathrm{LED}} R + V_{\mathrm{LED}} \tag{S1}$$

$$I_{\mathrm{LED}} = -I_{\mathrm{PV}} \tag{S2}$$

Moreover, from the detailed balance considerations, assuming that both the LED and the PV cell are ideal, i.e., the nonradiative recombination rates are zero, and assuming also that there are no photon exchange with any other objects, we have (2)

$$F_{\mathrm{PV}\to\mathrm{LED}} - F_{\mathrm{LED}\to\mathrm{PV}} + I_{\mathrm{LED}} / q = 0 \tag{S3}$$

and

$$F_{\mathrm{LED}\to\mathrm{PV}} - F_{\mathrm{PV}\to\mathrm{LED}} + I_{\mathrm{PV}} / q = 0 \tag{S4}$$

We see that Eq. (S3) and Eq. (S4) are in fact the same. For this configuration, under the ideal condition, there are therefore only three independent equations. With Eqs. (S1), (S2), and (S3), the steady state of the circuit satisfies

$$\frac{V_{\mathrm{PV}} - V_{\mathrm{LED}}}{qRA_{\mathrm{PV}}} = F_0\left(T_{\mathrm{LED}}, 0\right)\exp\left(\frac{V_{\mathrm{LED}}}{V_{\mathrm{th,LED}}}\right) - F_0\left(T_{\mathrm{PV}}, 0\right)\exp\left(\frac{V_{\mathrm{PV}}}{V_{\mathrm{th,PV}}}\right) \tag{S5}$$

Since $F_0\left(T_{\mathrm{LED}}, 0\right) > F_0\left(T_{\mathrm{PV}}, 0\right)$, for each value of V_{LED}, one can find a solution of V_{PV} in the range of $V_{\mathrm{PV}} > V_{\mathrm{LED}}$. Therefore, the system of Eqs. (1)-(3) admits an infinite number of possible solutions (1). Green (1) proposed that the steady state reached by the system will be that of minimum entropy production (3). In the following, we show that the physical steady state of this system can be determined by including nonradiative terms, and by taking the appropriate limit where these terms approach zero.

With nonradiative processes in the diodes, the detailed balance considerations result in:

$$F_{\mathrm{PV}\to\mathrm{LED}} - F_{\mathrm{LED}\to\mathrm{PV}} + N_{\mathrm{LED}}(0) - N_{\mathrm{LED}}(V_{\mathrm{LED}}) + I_{\mathrm{LED}}/q = 0 \tag{S6}$$

and

$$F_{\mathrm{LED}\to\mathrm{PV}} - F_{\mathrm{PV}\to\mathrm{LED}} + N_{\mathrm{PV}}(0) - N_{\mathrm{PV}}(V_{\mathrm{PV}}) + I_{\mathrm{PV}}/q = 0 \tag{S7}$$

In the above two equations, $N(0)$ and $N(V)$ are the nonradiative generation and recombination rates of the electron-hole pairs, respectively. For concreteness, we assume a Shockley-Read-Hall type of nonradiative recombination rate $N(V) = N(0)\exp(V/V_{\mathrm{th}})$ (2). The derivations and conclusions hold for other types of non-radiative recombination mechanisms.

From Eqs. (S6), (S7), and (S2), we obtain a relationship between the terms representing nonradiative recombination processes.

$$N_{\mathrm{LED}}(0)\left[1-\exp\left(\frac{V_{\mathrm{LED}}}{V_{\mathrm{th,LED}}}\right)\right] = N_{\mathrm{PV}}(0)\left[\exp\left(\frac{V_{\mathrm{PV}}}{V_{\mathrm{th,PV}}}\right)-1\right] \tag{S8}$$

Eq. (S8) provides an additional constraint on V_{LED} and V_{PV}. Thus, the system of equations (Eqs. (S1), (S2), (S7), (S8)) can admit a unique solution of steady state. The existence of a unique solution remains true even in the limit where $N_{\mathrm{LED}}(0) \to 0$ and $N_{\mathrm{PV}}(0) \to 0$. However, the solution in this limit depends on the ratio $N_{\mathrm{LED}}(0)/N_{\mathrm{PV}}(0)$ as both non-radiative rates go to zero.

An immediate observation from Eq. (S8) is that if V_{LED} and V_{PV} both are nonzero, they need to be of different signs. This requirement implies that the circuit in Fig. S1 does not operate as a self-sustaining thermophotonic circuit, where both V_{LED} and V_{PV} must be positive. With Eq. (S8), we can further show that the steady state of the circuit approaches that of a thermophotovoltaic system or negative-illumination system in the limiting cases where either of the nonradiative terms approaches zero. In the case when $N_{\mathrm{LED}}(0) \to 0$, but with $N_{\mathrm{PV}}(0) \neq 0$, Eq. (S8) yields $V_{\mathrm{PV}} = 0$. Thus, $V_{\mathrm{LED}} = -I_{\mathrm{LED}}R$, where $I_{\mathrm{LED}} = q\left[F_{\mathrm{LED}\to\mathrm{PV}} - F_{\mathrm{PV}\to\mathrm{LED}}\right]$. Since I_{LED} is

positive, V_{LED} has to be negative. Thus the LED in fact operates under the negative illumination condition (4), and generates electric power. The PV cell is shorted and thus not consuming or producing power. The system operates like a negative-illumination power generation system (4-7). Similarly, one can show that if $N_{\mathrm{PV}}(0) \to 0$, but $N_{\mathrm{LED}}(0) \neq 0$, then $V_{\mathrm{LED}} = 0$ and the system operates as a traditional thermophotovoltaic system.

Session II: Derivation of Eqs. (14) and (15) in the main text

For the system in Fig. 3b in the main text, all the LED's have the same voltage V_{LED}, and all the PV cells have the same voltage V_{PV}. Therefore, based on Eq. (7) in the main text, one has

$$\frac{I_{\mathrm{PV}}}{q} = \sum_j \left[A_{\mathrm{PV}} f_{\mathrm{PV},i\to\mathrm{LED},j} F_0\left(T_{\mathrm{PV}}, V_{\mathrm{PV}}\right) - A_{\mathrm{LED}} f_{\mathrm{LED},j\to\mathrm{PV},i} F_0\left(T_{\mathrm{LED}}, V_{\mathrm{LED}}\right) \right] \tag{S9}$$

In Eq. (S9), A_{LED} is the area of an LED. We assume the system is reciprocal, therefore, one has

$$A_{\mathrm{PV}} f_{\mathrm{PV},i\to\mathrm{LED},j} = A_{\mathrm{LED}} f_{\mathrm{LED},j\to\mathrm{PV},i} \tag{S10}$$

Substituting Eq. (S10) into Eq. (S9), we have

$$\begin{aligned} \frac{I_{\mathrm{PV}}}{q} &= \sum_j A_{\mathrm{PV}} f_{\mathrm{PV},i\to\mathrm{LED},j} \left[F_0\left(T_{\mathrm{PV}}, V_{\mathrm{PV}}\right) - F_0\left(T_{\mathrm{LED}}, V_{\mathrm{LED}}\right) \right] \\ &= A_{\mathrm{PV}} \left[F_0\left(T_{\mathrm{PV}}, V_{\mathrm{PV}}\right) - F_0\left(T_{\mathrm{LED}}, V_{\mathrm{LED}}\right) \right] \sum_j f_{\mathrm{PV},i\to\mathrm{LED},j} \\ &= A_{\mathrm{PV}} \left[F_0\left(T_{\mathrm{PV}}, V_{\mathrm{PV}}\right) - F_0\left(T_{\mathrm{LED}}, V_{\mathrm{LED}}\right) \right] \end{aligned} \tag{S11}$$

We obtain Eq. (14) in the main text. Similarly, based on Eq. (8) in the main text, one has

$$\begin{aligned}\frac{I_{\mathrm{LED}}}{q} &= \sum_i \left[A_{\mathrm{LED}} f_{\mathrm{LED},j\to\mathrm{PV},i} F_0\left(T_{\mathrm{LED}}, V_{\mathrm{LED}}\right) - A_{\mathrm{PV}} f_{\mathrm{PV},i\to\mathrm{LED},j} F_0\left(T_{\mathrm{PV}}, V_{\mathrm{PV}}\right)\right] \\ &= \sum_i A_{\mathrm{LED}} f_{\mathrm{LED},j\to\mathrm{PV},i} \left[F_0\left(T_{\mathrm{LED}}, V_{\mathrm{LED}}\right) - F_0\left(T_{\mathrm{PV}}, V_{\mathrm{PV}}\right)\right] \\ &= \left[F_0\left(T_{\mathrm{LED}}, V_{\mathrm{LED}}\right) - F_0\left(T_{\mathrm{PV}}, V_{\mathrm{PV}}\right)\right] A_{\mathrm{LED}} \sum_i f_{\mathrm{LED},j\to\mathrm{PV},i}\end{aligned} \tag{S12}$$

Based on reciprocity and the geometry of the circuit, we have

$$A_{\mathrm{LED}} \sum_i f_{\mathrm{LED},j\to\mathrm{PV},i} = A_{\mathrm{PV}} \sum_i f_{\mathrm{PV},i\to\mathrm{LED},j} = \frac{M}{N} A_{\mathrm{PV}} \tag{S13}$$

Substituting Eq. (S13) into Eq. (S12), one has

$$\frac{I_{\mathrm{LED}}}{q} = \frac{M}{N} A_{\mathrm{PV}} \left[F_0\left(T_{\mathrm{LED}}, V_{\mathrm{LED}}\right) - F_0\left(T_{\mathrm{PV}}, V_{\mathrm{PV}}\right)\right] \tag{S14}$$

We obtain Eq. (15) in the main text.

Session III: Effect of external quantum efficiencies

We quantify the effect of the external quantum efficiencies (EQE) in this session. In Fig. S2, we show the maximum power density and the maximum efficiency of the system as a function of the EQE for the LED's and the PV cells for two cases. The left column is for $M = 200$ and $N = 202$, where the required EQE for both LED's and PV cells needs to be greater than 99% for the system to generate power. In the case on the right where $M = 200$ and $N = 220$, the required EQE needs to be greater than 90%. We see that the best performance requires both the LED's and the PV cells have high EQE.

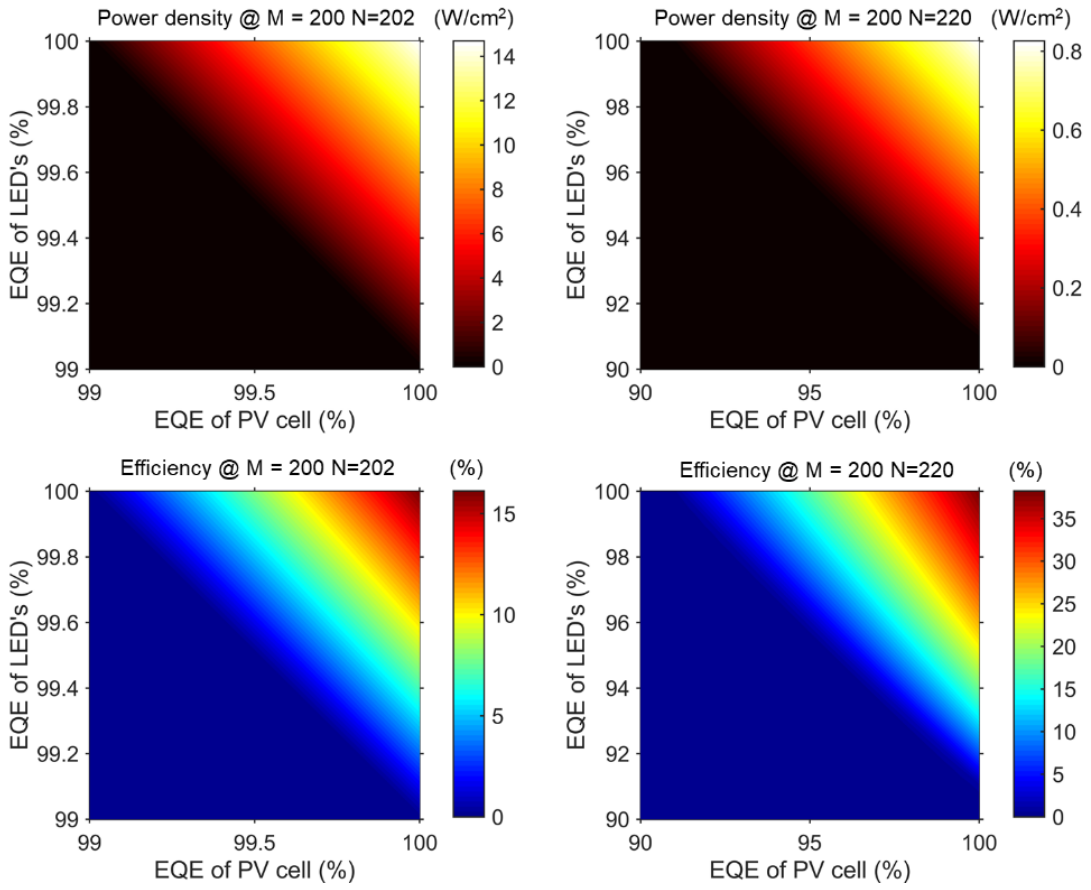

Fig. S2 Maximum power density and maximum efficiency of the proposed circuit as a function of the EQE of the PV cells and the LED's. (a) Maximum power density @ $M = 200$ and $N = 202$, (b) Maximum power density @ $M = 200$ and $N = 220$, (c) Maximum efficiency @ $M = 200$ and $N = 202$, and (d) Maximum efficiency @ $M = 200$ and $N = 220$.

Since the circuit requires the LED to operate in high temperature, we quantify the temperature effect on the external quantum efficiency next, by using the high-performance LED design in Ref. (8) as an example. We model the temperature dependence of the radiative and nonradiative properties based on the parameters and equations in the paper and Ref. (9). Since light extraction can be greatly enhanced by techniques such as near-field enhancement, we assume the light extraction is perfect. At 263 K, such a diode has an EQE of 99.87%, which is the same as the one shown in Fig. 3 of Ref. (8). As the temperature increase, this model predicts that the external quantum efficiency can stay above 90% for temperature below about 1200 K. Therefore,

for waste heat temperature regime discussed in the manuscript, the diodes can be efficient enough to allow power generation.

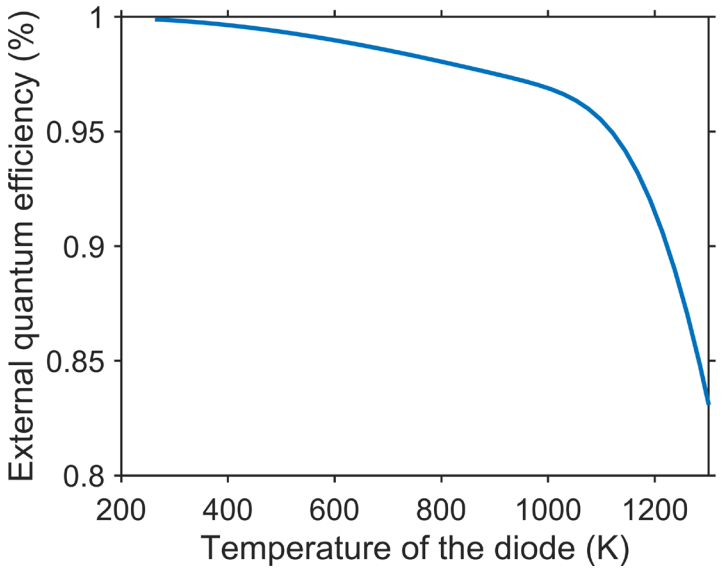

Fig. S3 Maximum external quantum efficiency of a GaAs diode as a function of temperature.

Session IV: The Near-field Enhancement Effect

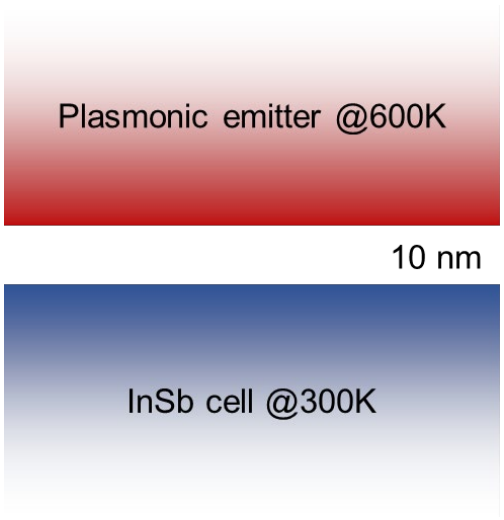

Fig. S4 Schematic of a near-field thermophotovoltaic with a plasmonic emitter and an InSb cell.

We make a comparison of the maximum power density of our thermophotonic circuit with an optimal near-field thermophotovoltaic system. With a heat source at 600 K, an effective approach to get a high-power density in near-field thermophotovoltaic is to use a low-bandgap cell and a plasmonic emitter that supports surface plasmon polariton with its frequency slightly above the bandgap, as suggested in (10, 11). Therefore, as shown in Fig. S4, we choose InSb as the cell for its low bandgap (0.17 eV) and a plasmonic emitter with its dielectric function described by a free-electron Drude model $\varepsilon(\omega) = 1 - \omega_p^2 \Big/ \left(\omega^2 + i\omega\Gamma\right)$, where ω_p and Γ are the plasma frequency and damping rate, respectively. The optical properties of the cell are obtained from Ref. (10). To maximize the power density, we assume the cell is ideal without any nonradiative recombination. The emitter and the cell are sufficient thick so that there is no leakage of photons on the backsides, and the gap between them has a size of 10 nm.

With this setup, we optimize ω_p and Γ simultaneously and achieve a maximum power density 14.4 W/cm^2 when $\omega_p =$ 0.35 eV and Γ = 8.3 meV. This power density is about the same with the maximum power density we demonstrated using a *far-field* thermophotonic system in the manuscript. With a similar near-field enhancement effect, i.e., by placing the LED's and PV cells 10 nm apart, our calculations show that a power density of 114 W/cm^2 is achievable, which is significantly larger than that of the near-field thermophotovoltaic system. We note that the power density of 114 W/cm^2 is obtained assuming a bandgap of 1.64 eV (AlGaAs ternary system). This power density can be further increased by using a larger-bandgap semiconductor like GaN. Therefore, the thermophotonic system can achieve significantly higher power density then thermophotovoltaic systems.

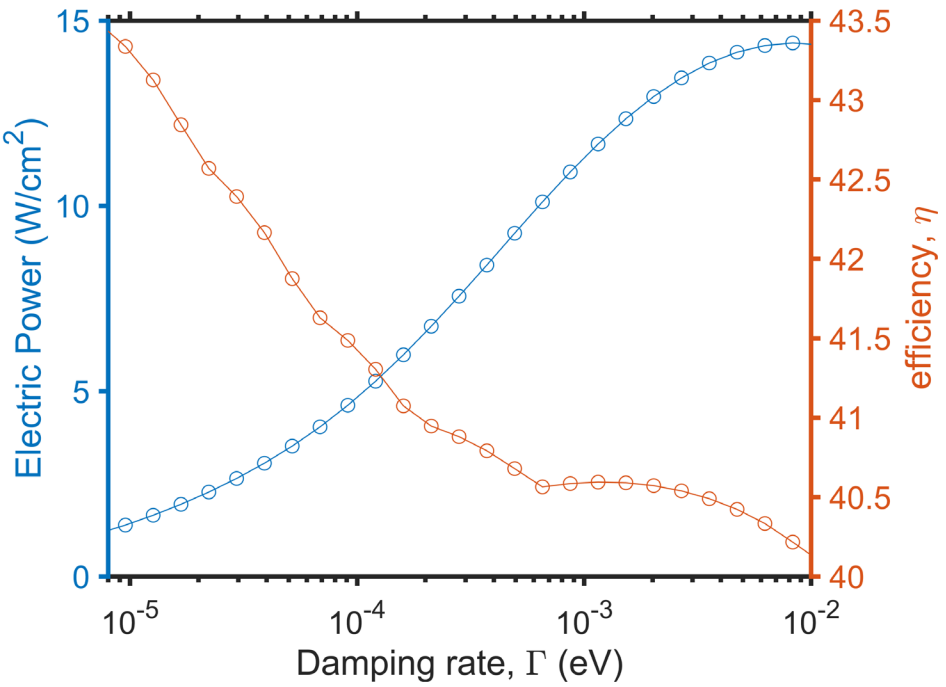

Fig. S5 Maximum efficiency and power density of the near-field thermophotovoltaic system in Fig. S4 as a function of the damping rate.

We would like to point out that, the maximum power density of the thermophotonic circuit decreases as the efficiency of the system increases, as can be seen from as shown in Fig. 4(a) in the main text. And this is also true for thermophotovoltaic systems. We can take the near-field thermophotovoltaic system in Fig. S4 as an example. One can improve the efficiency of the system by decreasing the damping rate in the Drude model since it will make the bandwidth of the surface plasmons narrower. However, the power density would also decrease simultaneously. To show this effect, we fix ω_p at 0.35 eV and decrease the damping rate from the peak-power configuration. For each case, we calculate the maximum power density and efficiency of the near-field TPV system, and the results are shown in Fig. S5. We see that the efficiency increases from 40.2% to 43.5%, but the power density drops significantly from 14.4 to 1.4 W/cm^2. Therefore, in practical

design of thermophotonic system, there would be a tread-off between efficiency and power density, just as other heat engines.

References

1. Green MA (2006) *Third Generation Photovoltaics: Advanced Solar Energy Conversion* (Springer Science & Business Media, New York).
2. Shockley W, Queisser HJ (1961) Detailed balance limit of efficiency of p-n junction solar cells. *J Appl Phys* 32:510-519.
3. de Groot SR, Mazur P (1984) *Non-Equilibrium Thermodynamics* (Dover Publications, New York).
4. Santhanam P, Fan S (2016) Thermal-to-electrical energy conversion by diodes under negative illumination. *Phys Rev B* 93:161410.
5. Lin C, Wang B, Teo K, Zhang Z (0800) A coherent description of thermal radiative devices and its application on the near-field negative electroluminescent cooling. *Energy* 147:177-186.
6. Hsu W-C, et al. (2016) Entropic and near-field improvements of thermoradiative cells. *Sci Rep* 6:34837.
7. Buddhiraju S, Santhanam P, Fan S (2018) Thermodynamic limits of energy harvesting from outgoing thermal radiation. *Proc Natl Acad Sci* 115:E3609-E3615.
8. Xiao TP, Chen K, Santhanam P, Fan S, Yablonovitch E (2018) Electroluminescent refrigeration by ultra-efficient GaAs light-emitting diodes. *J Appl Phys* 123:173104.
9. Heikkilä O, Oksanen J, Tulkki J (2009) Ultimate limit and temperature dependency of light-emitting diode efficiency. *J Appl Phys* 105:093119.
10. Ilic O, Jablan M, Joannopoulos JD, Celanovic I, Soljačić M (2012) Overcoming the black body limit in plasmonic and graphene near-field thermophotovoltaic systems. *Opt Express* 20:A366-A384.
11. Zhao B, et al. (2017) High-performance near-field thermophotovoltaics for waste heat recovery. *Nano Energy* 41:344-350.